

A Population of Multipotent CD34-Positive Adipose Stromal Cells Share Pericyte and Mesenchymal Surface Markers, Reside in a Periendothelial Location, and Stabilize Endothelial Networks

Dmitry O. Traktuev, Stephanie Merfeld-Clauss, Jingling Li, Mikhail Kolonin, Wadih Arap, Renata Pasqualini, Brian H. Johnstone and Keith L. March

Circ. Res. 2008;102;77-85; originally published online Oct 25, 2007;

DOI: 10.1161/CIRCRESAHA.107.159475

Circulation Research is published by the American Heart Association, 7272 Greenville Avenue, Dallas, TX 75214

Copyright © 2008 American Heart Association. All rights reserved. Print ISSN: 0009-7330. Online ISSN: 1524-4571

The online version of this article, along with updated information and services, is located on the World Wide Web at:

<http://circres.ahajournals.org/cgi/content/full/102/1/77>

Data Supplement (unedited) at:

<http://circres.ahajournals.org/cgi/content/full/CIRCRESAHA.107.159475/DC1>

Subscriptions: Information about subscribing to Circulation Research is online at
<http://circres.ahajournals.org/subscriptions/>

Permissions: Permissions & Rights Desk, Lippincott Williams & Wilkins, a division of Wolters Kluwer Health, 351 West Camden Street, Baltimore, MD 21202-2436. Phone: 410-528-4050. Fax: 410-528-8550. E-mail:
journalpermissions@lww.com

Reprints: Information about reprints can be found online at
<http://www.lww.com/reprints>

A Population of Multipotent CD34-Positive Adipose Stromal Cells Share Pericyte and Mesenchymal Surface Markers, Reside in a Periendothelial Location, and Stabilize Endothelial Networks

Dmitry O. Traktuev, Stephanie Merfeld-Clauss, Jingling Li, Mikhail Kolonin, Wadih Arap, Renata Pasqualini, Brian H. Johnstone, Keith L. March

Abstract—It has been shown that stromal–vascular fraction isolated from adipose tissues contains an abundance of CD34⁺ cells. Histological analysis of adipose tissue revealed that CD34⁺ cells are widely distributed among adipocytes and are predominantly associated with vascular structures. The majority of CD34⁺ cells from freshly isolated stromal–vascular fraction were CD31[−]/CD144[−] and could be separated from a distinct population of CD34⁺/CD31⁺/CD144⁺ (endothelial) cells by differential attachment on uncoated plastic. The localization of CD34⁺ cells within adipose tissue suggested that the nonendothelial population of these cells occupied a pericytic position. Analysis of surface and intracellular markers of the freshly isolated CD34⁺/CD31[−]/CD144[−] adipose-derived stromal cells (ASCs) showed that >90% coexpress mesenchymal (CD10, CD13, and CD90), pericytic (chondroitin sulfate proteoglycan, CD140a, and CD140b), and smooth muscle (α -actin, caldesmon, and calponin) markers. ASCs demonstrated polygonal self-assembly on Matrigel, as did human microvascular endothelial cells. Coculture of ASCs with human microvascular endothelial cells on Matrigel led to cooperative network assembly, with enhanced stability of endothelial networks and preferential localization of ASCs on the abluminal side of cords. Bidirectional paracrine interaction between these cells was supported by identification of angiogenic factors (vascular endothelial growth factor, hepatocyte growth factor, basic fibroblast growth factor), inflammatory factors (interleukin-6 and -8 and monocyte chemoattractant protein-1 and -2), and mobilization factors (macrophage colony-stimulating factor and granulocyte/macrophage colony-stimulating factor) in media conditioned by CD34⁺ ASCs, as well a robust mitogenic response of ASCs to basic fibroblast growth factor, epidermal growth factor, and platelet-derived growth factor-BB, factors produced by endothelial cells. These results demonstrate for the first time that the majority of adipose-derived adherent CD34⁺ cells are resident pericytes that play a role in vascular stabilization by mutual structural and functional interaction with endothelial cells. (*Circ Res.* 2008;102:77-85.)

Key Words: adipose stromal cells ■ pericytes ■ growth factors/cytokines

Over the past decade, interest has grown in identifying and characterizing progenitor cells isolated from a range of types of adult tissues, such as subtypes of endothelial progenitor cells,^{1–4} bone marrow–derived mesenchymal cells,^{1,5,6} and satellite cells from skeletal muscles.^{7–10} Experimental models and clinical trials have shown that these cells stimulate angiogenesis in ischemic tissues and may preserve or rescue cardiac and brain function in the context of ischemic insult. Despite potentially significant therapeutic effects demonstrated by a majority of these cell types, their relatively limited availability in adult organisms (endothelial progenitor cells and mesenchymal stem cells [MSCs]) or invasive nature of their procedures of their harvest (MSCs and myoblasts) may pose a challenge to their extensive clinical application.

Accordingly, adipose-derived stromal cells (ASCs), which can be obtained in abundance through minimally invasive harvest procedures (lipoaspiration or abdominoplasty), present an important alternative for autologous cell transplantation.

Recently it has been shown that the ASC population, which includes cells that function as adipocyte progenitors (preadipocytes),¹¹ contains cells able to differentiate in vitro into multiple mesenchymal cell types^{12–16} as well as hepatocytes,¹⁷ neuronal cells,¹⁸ endothelial cells (ECs),^{19,20} and cardiomyocytes.^{21,22} In addition, locally or systemically injected ASCs, whether freshly isolated or expanded, stimulate angiogenesis and mediate recovery of muscle tissues following ischemic insult.^{19,22–26}

Original received December 20, 2006; resubmission received July 9, 2007; revised resubmission received October 1, 2007; accepted October 15, 2007. From the Indiana Center for Vascular Biology and Medicine (D.O.T., S.M.-C., J.L., B.H.J., K.L.M.), Indiana University School of Medicine, Indianapolis; M. D. Anderson Cancer Center (M.K., W.A., R.P.), University of Texas, Houston; and R. L. Roudebush Veterans Affairs Medical Center (K.L.M.), Indianapolis, Ind.

Correspondence to Keith L. March, MD, PhD, Indiana Center for Vascular Biology & Medicine, 975 W Walnut St, IB 441, Indianapolis, IN 46202. E-mail kmarch@iupui.edu

© 2008 American Heart Association, Inc.

Circulation Research is available at <http://circres.ahajournals.org>

DOI: 10.1161/CIRCRESAHA.107.159475

Despite the plasticity of ASCs *in vitro*, and their effects in experimental models *in vivo*, there is little knowledge of their natural localization, characteristics, and physiologic role(s) *in vivo*. Initial enzymatic liberation of ASCs yields a mixture of stromal and vascular cells (referred to as the stromal-vascular fraction [SVF]), indicating a spatial proximity. Several studies have examined surface marker profiles of the ASC population within the SVF and have observed that the total nonendothelial population is highly enriched for CD34-expressing cells.^{19,23,24}

This study was designed to define the *in vivo* localization of CD34⁺ ASCs in adipose tissue and to further characterize their phenotype with respect to expression of surface markers and factors important for intracellular interactions, to help uncover their normal physiological functions, and to shed further light on their angiogenic properties.

To this end, we demonstrate, for the first time, the existence of a periendothelial subpopulation of ASCs that bear many hallmarks of pericytes and provide vascular stability through functional interaction with ECs. This information may help to delineate both their capabilities and limitations with respect to their potential clinical translation.

Materials and Methods

Isolation and Culture of Human ASCs

Human subcutaneous adipose tissue samples (N=10), obtained from lipoaspiration/liposuction procedures were digested in collagenase type I solution (Worthington Biochemical, Lakewood, NJ) under agitation for 2 hours at 37°C and centrifuged at 300g for 8 minutes to separate the stromal cell fraction (pellet) from adipocytes. The pellet was resuspended in DMEM/F12 containing 10% FBS (Hyclone, Logan, Utah) filtered through 250- μ m Nitex filters (Sefar America Inc, Kansas City, Mo) and centrifuged at 300g for 8 minutes. The cell pellet was treated with red cell lysis buffer (154 mmol/L NH₄Cl, 10 mmol/L KHCO₃, 0.1 mmol/L EDTA) for 10 minutes. The final pellet was resuspended in EBM-2/5% FBS or EGM2-MV (Cambrex, Baltimore, Md).

Flow Cytometric Characterization of Human ASCs

Freshly isolated SVF cells, and cells cultured for 2 days on culture plastic, were analyzed for surface marker expression using a Calibur flow cytometer analyzer and Cell QuestPro software (Becton Dickinson Immunocytometry Systems). Day 2 cells were harvested with 2 mmol/L EDTA/PBS. All of the following steps were performed on ice. Cell pellets were incubated for 20 minutes with primary antibodies or matching isotype controls (5 μ g/mL). The primary antibodies used were CD10-phycoerythrin (PE), CD13-PE, CD31-PE, CD45-fluorescein isothiocyanate, CD34-allophycocyanin, CD90-PE, CD140a-PE, CD140b-PE, CD144-PE, and chondroitin sulfate proteoglycan (NG2) (Chemicon, Temecula, Calif). To detect nonlabeled primary antibodies, samples were incubated for 20 minutes with PE-conjugated antibodies (BD, San Diego, Calif), then washed with 2% FBS/PBS, and fixed with 2% paraformaldehyde.

Immunofluorescent Analysis of Adipose Tissue

Frozen sections of human fat tissue were simultaneously stained with rabbit anti-CD31 and mouse anti-human CD34 or with mouse anti-human CD31 and rabbit anti-CD140b antibodies. See the online data supplement, available at <http://circres.ahajournals.org>, for detailed procedures.

Immunofluorescent Analysis of Isolated ASCs

Freshly isolated ASCs were stained by immunofluorescence, 3 days after plating, against caldesmon, calponin, and α -smooth muscle actin antigens. See the online data supplement for detailed procedures.

Matrigel Assay

Human microvascular ECs (HMVECs) (passage 7) and ASCs (day 2 or passage 1) were labeled with PKH2 (green) and PKH-26 (red) (Sigma, St Louis, Mo), respectively. Twelve-well plates were coated with 600 μ L per well of growth factor-reduced Matrigel (BD). Plates were incubated at 37°C for 2 hours. Cells (10⁵ cells/well). HMVECs and ASCs were plated separately or together at a ratio of 1:3 (7.5 \times 10⁴ HMVECs+2.5 \times 10⁴ ASCs) in 600 μ L of DMEM/10% FBS and were cultured at 37°C with 10% CO₂ and monitored frequently by fluorescent microscopy.

Generation of Conditioned Media

Human (h)ASCs and HMVECs were grown in EGM-2MV, in T75 flasks, until confluent, and media were changed to 10 mL of EBM-2/5% FBS. Seventy-two hours later, conditioned media (CM) was collected, centrifuged at 300g for 5 minutes, and frozen at -80°C. Cell counts were determined in a standard manner.

Proliferation Assay

Cells were grown for 24 hours in EBM-2/5% FBS before detachment with 0.05% trypsin/EDTA and replating into 12-well plates at 10⁴ cells per well. Four hours postplating, media were changed to fresh EBM-2/5% FBS (control) or CM prepared as above. Four days later, cells were detached and counted.

Migration Assay

The bottom surfaces of Costar Transwell insert membranes, with pore diameters of 5 μ m for ASCs and 8 μ m for HMVECs, were coated with 50 μ g/mL rat tail collagen I (BD). Cells (3 \times 10⁴) in 0.1 mL of EBM-2/5% FBS were added into each insert, and the inserts were placed into 24-well plates, with wells containing either controls or CM. Cells were allowed to migrate for 4 hours, after which the downward aspect of the inserts were stained for transmigratory cells with Diff-Quick (Dade Behring). Cells retained on the top surface of the membranes were eliminated using a cotton swab. Insert undersides were imaged and migratory cells quantitated using ImageJ software.

Evaluation of hASC Mitogenic Response to Individual Growth Factors

Freshly isolated ASCs were adhered on cell culture plastic for 2 days before harvesting attached cells with 0.05% trypsin/EDTA. Cells were seeded at 3 \times 10³ cells/cm² in 12-well plates and allowed to attach overnight in EBM-2/5% FBS medium, which was then replaced with EBM-2/5% FBS alone (control) or EBM-2/5% FBS supplemented with basic fibroblast growth factor (bFGF), epidermal growth factor (EGF), or platelet-derived growth factor (PDGF)-BB individually at final concentrations of 10 pg, 100 pg, 1 ng, or 10 ng each or the mixture of all of these, each at the specified concentration. Cells were cultured for 4 days, with a medium change after 48 hours, and then detached using 0.05% trypsin/EDTA, and viable cells were counted using a hemacytometer and trypan blue. Proliferation data are presented as the ratio of cells per well supplemented with growth factor to cells per well in control media.

See the online data supplement for detailed information regarding analysis of factor accumulation in CM of hASC and HMVECs, quantitative assessment of growth factors accumulated in HMVEC CM, and statistical analysis.

Results

Defining the Subpopulation of SVF Corresponding to ASCs

The objective of this study was to define the location of ASCs within adipose tissues. Initially, it was necessary to carefully

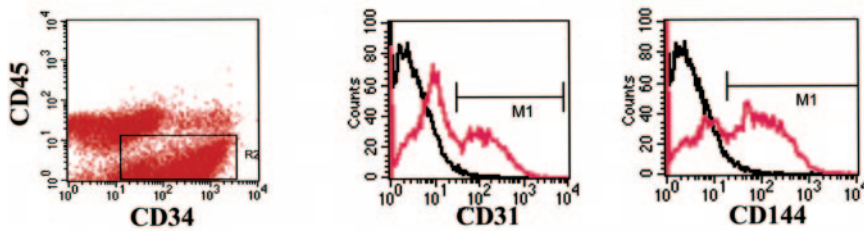
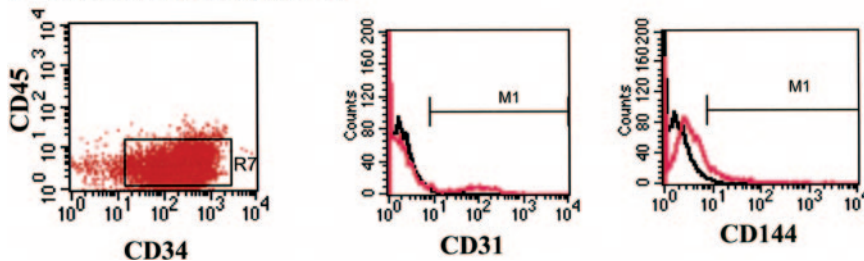
A Stromal - Vascular fraction**B Attached cells (day 2-3)**

Figure 1. Fluorescence-activated cell sorting analyses of SVF of adipose tissue. Analysis of cells, either freshly isolated or adherently cultured for 2 days, was performed using CD34 (allophycocyanin), CD45 (fluorescein isothiocyanate), CD144 (PE), and CD31 (PE) antibodies. Cell populations in flow cytometric gates outlined by black boxes (R2 and R7), representing CD34⁺/CD45⁻ populations, were evaluated for the presence of ECs (CD144⁺/CD31⁺). Signals for fluorescent isotype IgG are shown as black and antigen-specific signals are shown as red curves.

define the phenotype of the ASC subpopulation contained within the mixed population comprising SVF. Multilabel flow cytometric analysis was performed using markers that allowed differentiation among 3 main cell types: ASCs, ECs, and leukocytes. In addition, we used dissimilar attachment and growth properties to further distinguish these. Endothelial and leukocyte cells use protein matrices to promote attachment and growth in culture.²⁷⁻²⁹ A limited plating time (1 to 2 days) of SVF on uncoated tissue culture plastic resulted in selective adherence of a population that was greatly reduced in the percentage of endothelial (CD31 and CD144) and leukocytic (CD45) cells (Figure 1). Staining of freshly isolated cells for CD34 and CD45 revealed 3 major subpopulations: CD34⁻/CD45⁺, CD34⁺/CD45⁺, and CD34⁺/CD45⁻ (Figure 1a). The CD45⁺ cells (47.6±5.8% of SVF) likely include a mixture of leukocytes contained within vasculature as well as resident in the adipose tissue.^{11,30} Analysis of the CD34⁺/CD45⁻ population revealed a significant subpopulation (20±5%) that coexpressed the EC markers CD31 and CD144. Culturing isolated cells on plastic

resulted in enrichment to >85% of cells bearing the surface marker profile CD34⁺/CD31⁻/CD45⁻/CD144⁻ (Figure 1b). Accordingly, this adherent fraction of nonendothelial CD34⁺/CD31⁻/CD45⁻/CD144⁻ cells broadly defines the ASC population that has been previously characterized as pluripotent. The differentiation capacity of this purified population was confirmed by the demonstration that these undergo both osteogenesis and adipogenesis at high frequency (Figures I and II in the online data supplement).

CD34⁺ Cells in Adipose Tissue Are Associated With the Vasculature

Immunofluorescent analysis of human adipose tissue sections established that the majority of CD34⁺ cells were associated with vessels within the tissue (Figure 2). A significant portion of these cells also coexpressed CD31, and therefore were presumably capillary ECs. However, a separate and predominant population of CD34⁺ cells, which did not express CD31, was

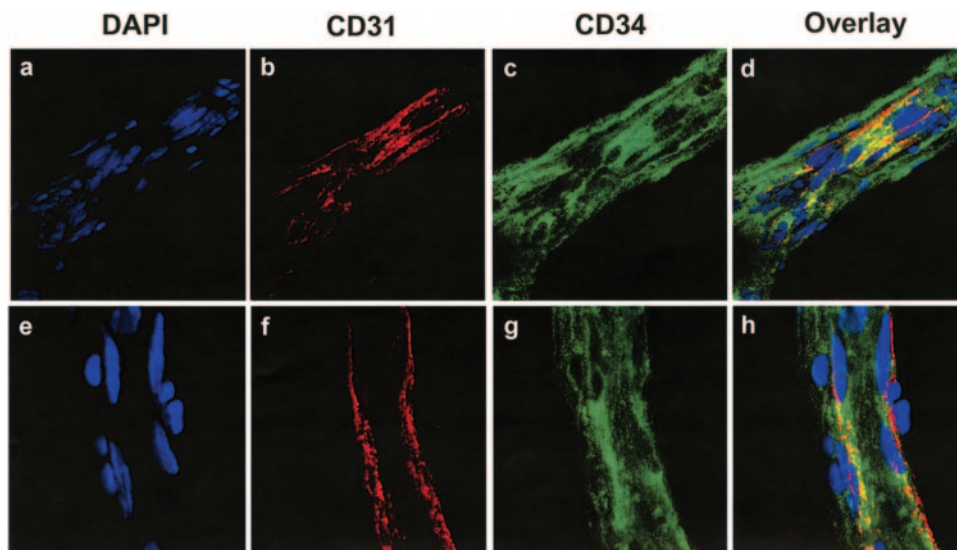


Figure 2. Histological analysis of human adipose tissue. Frozen sections of human fat were stained for the endothelial marker CD31 (red) and a major fresh ASC marker CD34 (green). Nuclei are revealed by 4',6'-diamidino-2-phenylindole (DAPI) staining.

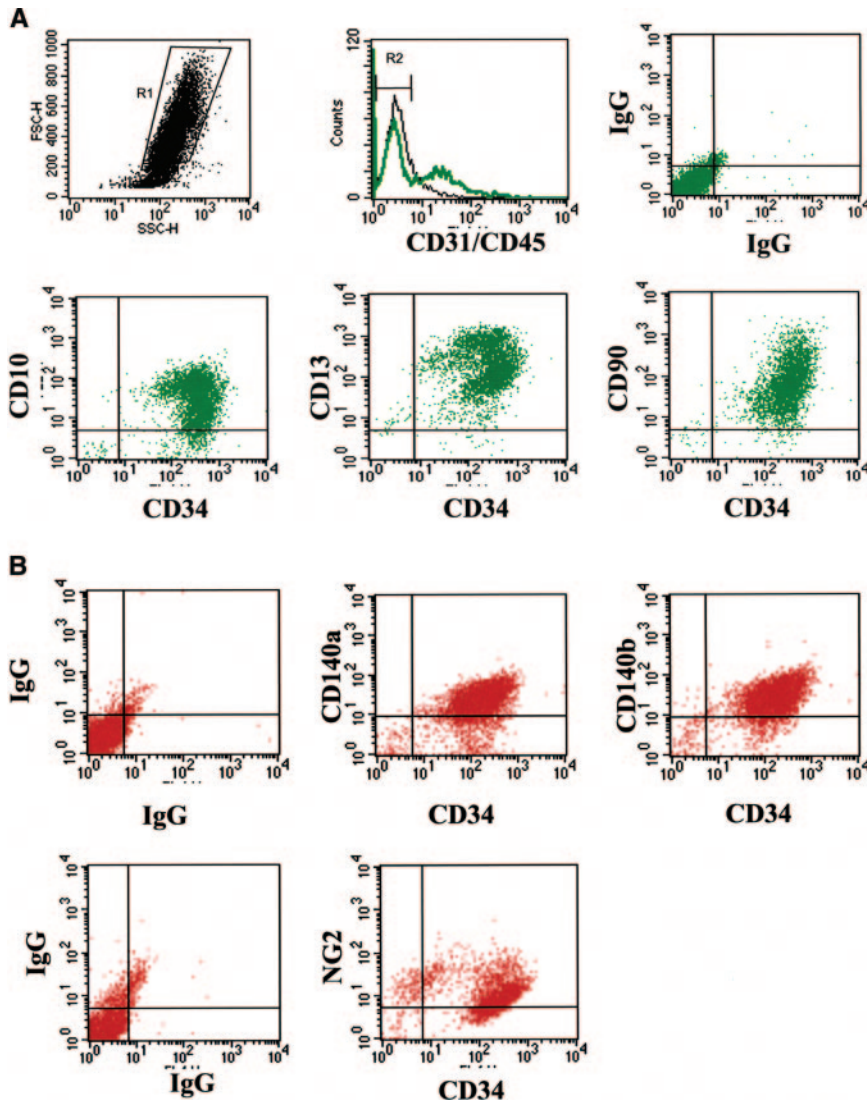


Figure 3. Fluorescence-activated cell sorting analysis of ASCs for coexpression of CD34 with mesenchymal (a) and pericyte (b) markers, assessed 2 days postadherence to plastic. Analysis was performed for CD34, CD45, CD10, CD13, CD90, CD140a, CD140b, NG2, and isotype IgGs.

observed in proximity to ECs. The perivascular location of the CD34⁺/CD31⁻ cells suggested their pericytic identity.

Adipose-Derived CD34⁺/CD31⁻ Cells Display Pericytic Markers In Vitro

The predominantly perivascular location of the CD34⁺/CD31⁻ cells suggested that these cells were pericytes, mural cells, which line and stabilize vascular endothelium *in vivo*.²⁷ The adherent CD34⁺/CD31⁻ population of SVF was thus characterized for expression of mesenchymal, pericytic, and smooth muscle cell markers. More than 95% of the adherent CD34⁺/CD45⁻/CD31⁻ population coexpressed the mesenchymal cell markers CD10, CD13, and CD90 (Figure 3a). Analysis of surface markers used to define pericytes^{28–30} (Figure 3b) revealed that the majority of the ASCs expressed chondroitin sulfate proteoglycan (NG2), CD140a, and CD140b (PDGF receptor- α and - β , respectively). Analysis of cytoskeletal markers performed by immunocytochemistry of freshly isolated ASCs revealed that many ASCs also expressed the smooth muscle cell antigens caldesmon, calponin, and α -smooth muscle actin (Figure 4).

The ASC antigen profile by flow cytometry was confirmed by PCR analysis of mRNA expression corresponding with multiple proteins (supplemental Figure III).

ASCs Occupy a Perivascular Position in Adipose Tissue In Vivo

The spatial relationship between EC and ASCs was evaluated by colabeling adipose tissue sections with antibodies specifically decorating each cell type. The surface antigen CD140b was highly expressed by ASCs (Figure 3b) but not microvascular EC (data not shown), whereas, as shown above, ASCs did not express the EC antigen CD31. Cells comprising capillary vessels in adipose tissue exhibited spatially separated expression of each antigen; CD31 (green) was specifically associated with cells forming the vessel lumen, whereas CD140b (red) was displayed on the surface of cells lining the exterior surface of the vessels (Figure 5). Taken together, these data demonstrate that ASCs are pericytic cells that occupy a perivascular position *in vivo*.

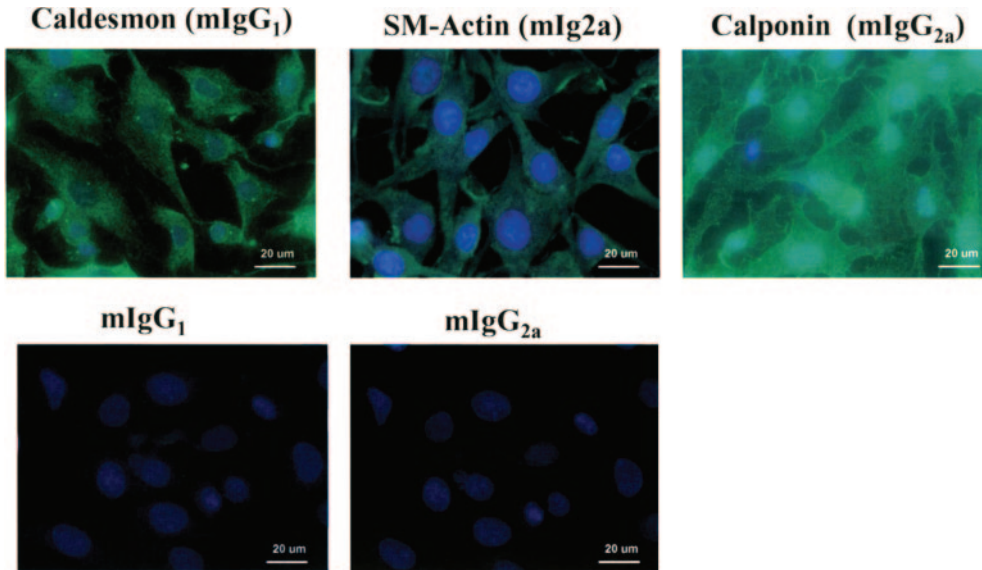


Figure 4. Immunocytochemistry of cytoskeletal antigens in ASCs 2 days postadherence to plastic. Formaldehyde-fixed cells were permeabilized and stained against α -smooth muscle actin, caldesmon, and calponin or with isotype-matched IgGs. Nuclei are revealed by DAPI staining.

ASCs Coassemble With and Stabilize Newly Forming EC Networks

To test for a functional correlate of the ASC–EC proximity in vascular structures, we evaluated the effect of ASCs on formation and stabilization of EC network on Matrigel. As shown in Figure 6a, HMVECs cultured in growth factor–free media form temporary networks that started dissociating after 24 hours. Plating ASCs alone also revealed formation of networks on Matrigel. However, coculturing HMVECs with

ASCs produced stabilized cell networks that remained intact for up to 5 days ($n=9$), when experiments terminated. Coculture of fluorescently labeled HMVECs and ASCs revealed that the cells formed a cooperative network of tubular structures on Matrigel matrix with HMVECs (green) forming the lumen and ASCs (red) overlaying tubes formed by HMVECs (Figure 6b). Extending this finding into an *in vivo* system, we found that subcutaneous implantation of collagen/fibronectin gels containing ASCs admixed with ECs into

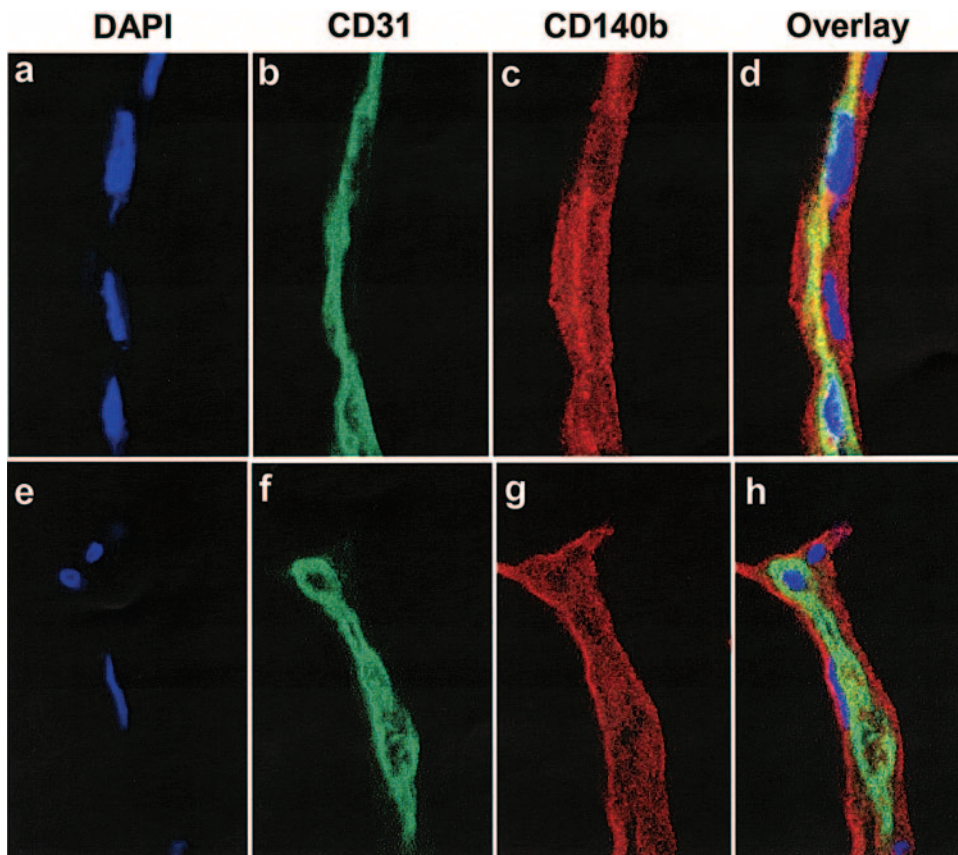


Figure 5. Histological analysis of human adipose tissue for microvascular endothelium and CD140b-expressing cells. Frozen sections of human fat were stained against endothelial CD31 (green) and ASC/pericyte CD140b (red) markers. Nuclei are revealed by DAPI staining.

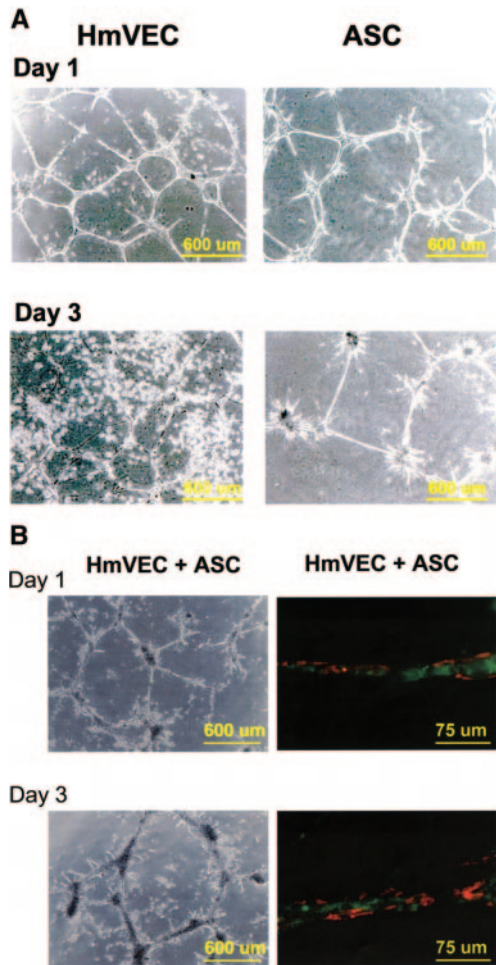


Figure 6. A, Evaluation of cord formation by HMVECs and hASCs on Matrigel surface. Cord formation was evaluated (phase contrast) on days 1 and 3 postplating. B, Fluorescent dye-labeled ECs (green) and hASCs (red) were mixed and plated on Matrigel. Cord formation was evaluated on days 1 and 3 postplating by fluorescence.

nude mice ($n=4$) also demonstrated formation of human-derived vascular structures with both endothelial and mural layers, with the mural layer comprising ASCs (supplemental Figure IV).

Paracrine Crosstalk Between ASCs and EC

To evaluate for paracrine crosstalk between ASCs and ECs, we evaluated the effects of CM collected from each of HMVECs and ASCs on the proliferation and migration of the complementary cell types. As is shown in Figure 7a, CM manifested strong mitogenic effects on ASCs. In 4-hour experiments, more than twice as many cells migrated through the filter in response to HMVEC CM as to control media EBM-2/5% FBS ($P<0.001$). In parallel with this chemotactic effect, HMVEC CM stimulated more than 3.5-fold expansion of ASCs compared with control media ($P<0.001$) (Figure 7b).

We evaluated the complementary effects of ASC-secreted factors on EC. Unlike the finding with EC CM, ASC CM did not stimulate proliferation to cell numbers above those originally seeded but rather demonstrated a strong pro-survival effect on microvascular EC, markedly limiting their

death in basal medium. As is shown in Figure 7d, HMVECs cultured in EBM-2/5% FBS for 4 days exhibit cell loss, with 50% remaining viable ($P<0.001$), whereas exposing cells to ASC CM (at 1:1 dilution) for the same time supports 100% cell survival ($P<0.001$). Evaluation for HMVEC chemotaxis toward ASC CM (Figure 7c) showed a modest but significant increase in migration compared with control media ($n=9$).

To evaluate factors responsible for such effects, we analyzed proteins secreted by freshly isolated ASCs and cultured HMVECs using antibody Arrays (RayBiotech). The protein profile in CM from ASCs revealed multiple angiogenic factors, including angiogenin, vascular endothelial growth factor, hepatocyte growth factor, bFGF, and β -nerve growth factor; the cytokines interleukin-6, -8, -11, and -17; and the cell-mobilizing factors monocyte chemoattractant proteins 1 and 2, granulocyte/macrophage colony-stimulating factor, and macrophage colony-stimulating factor (supplemental Figure Va and Vb). Notably absent were EGF, PDGF-BB, transforming growth factors, stromal cell-derived factor-1, and stem cell factor. See the online data supplement for all proteins detected, as well as their respective detection limits.

On the other hand, cultured HMVEC CM included multiple factors, such as bFGF, EGF, and PDGF-AA, -AB, and -BB (supplemental Figure Vc). Several of these were quite distinct, whereas a few overlapped with the profile of ASC secretion (eg, bFGF). Quantitative analysis revealed that in HMVEC CM (72 hours), the concentration of factors were as follows: EGF, 83.6 ± 51.0 pg/mL; bFGF, 243.0 ± 46.4 pg/mL; and PDGF-BB, 405.2 ± 85.0 pg/mL. The concentration of these in basal media before conditioning was below 2 pg/mL. The dose dependence of the effects of these factors on ASC proliferation was evaluated by the addition of each factor to basal medium. As shown in Figure 8, these factors exert strong mitogenic effects on ASCs over concentrations that overlap with those secreted by ECs. Further evaluation revealed synergy among factors with respect to mitogenesis of ASCs. We observed significantly higher mitogenesis of ASCs to the factor mixture compared with individual factors at concentrations of 100 pg/mL for bFGF ($P<0.05$) and PDGF-BB ($P<0.001$) and 1 ng/mL for EGF ($P<0.05$) and PDGF-BB ($P<0.01$).

Discussion

This study demonstrates for the first time that stromal cells derived from subcutaneous adipose tissue, which have properties of preadipocytes^{12,15,31} and manifest clonal pluripotency along multiple lineage pathways,^{15,32,33} serve structurally and functionally as pericytes within adipose tissue. This finding sheds a unique light on their importance in normal adipose biology as well as the biological basis for their ability to promote vascularization and accelerate tissue perfusion in the context of ischemia.

Our study shows the prominent and consistent presence of the marker CD34 on freshly isolated ASCs, occurring in the absence of CD45, which distinguishes ASCs from cells of hematopoietic lineage. The variability in reports of ASC as CD34⁺, as well as CD34⁻ cells,^{12,15,24} is likely a consequence of its consistent downregulation during culturing over a

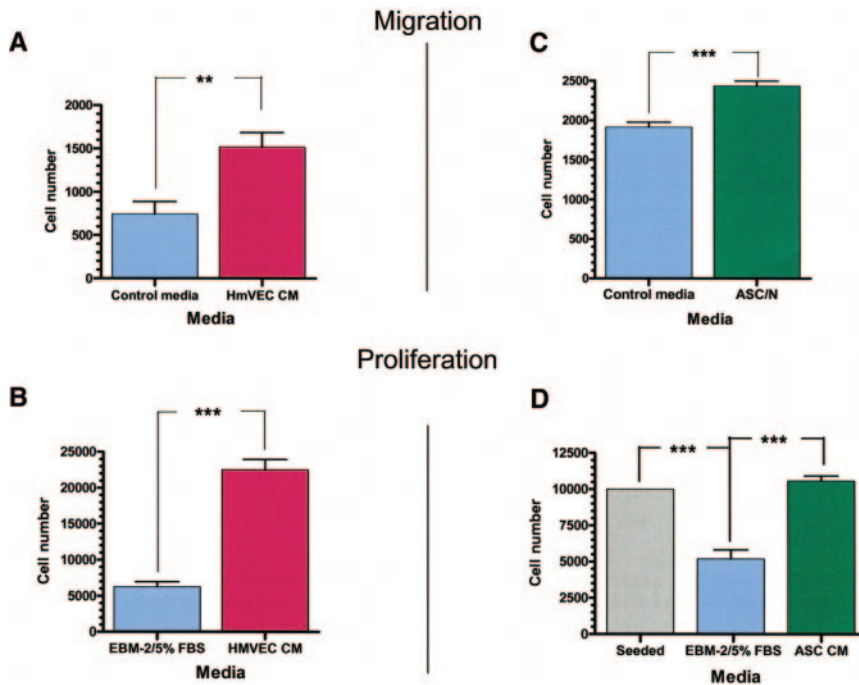


Figure 7. Effects of media conditioned for 72 hours by HMVECs (A and B) or ASCs (C and D) on ASC and HMVEC migration (A and C) and proliferation (B and D). The cells were added to collagen-coated Costar Transwell inserts and were allowed to migrate for 4 hours toward the lower wells containing control or CM (migration). The attached cells were exposed to either control or CM for 4 days and were detached and counted subsequently (proliferation).

several-day period²⁴; passaged ASCs have been characterized as CD34^{low} or CD34⁻.^{12,15,24} We have found that CD34 antigen serves as a convenient tool for identifying the majority of freshly isolated ASCs, when used with the CD45⁻ and CD31⁻ phenotypes to exclude leukocytic and endothelial populations respectively.

This study also demonstrates that the marker profile of ASCs shares much in common with bone marrow-derived MSCs, as also found in analyses of gene expression.^{34–36} One apparent distinction is a widespread and prominent degree of CD34 expression on ASCs, contrasting with descriptions of MSCs as lacking CD34.^{37–39} Based on our observation that ASC expression of CD34 is rapidly downregulated in culture,²⁴ and that most isolation protocols for MSCs require

extended culture periods before availability of MSCs for study, we hypothesize that MSC in situ may indeed express the CD34 antigen but this property is lost during expansion between isolation and surface marker evaluation. Indeed, early descriptions of MSCs reported enrichment of their colony-forming activity using CD34⁺ selection⁴⁰

ASCs Express Pericyte Markers

The perivascular location of CD34⁺/CD31⁻ cells suggested a pericytic identity, which was confirmed by flow cytometry and further immunolocalization of these cells using a panel of markers associated with pericytes, including CD140a and CD140b (PDGF receptor- α and - β), and NG2. Staining for these markers in adipose tissue confirmed a perivascular location for the ASC population. It is notable that these markers were present on most ASCs, as defined above (>95%), reflecting that pericytic cells are not a minor subset of ASCs isolated using standard methods but rather are substantially identical to these cells, at least in subcutaneous adipose tissue.

ASCs and Endothelial Cells Are Linked by Physical and Paracrine Interactions

Exploration of the relationship of ASCs with ECs clearly revealed their capacity for both structural and functional interactions. ASCs and EC in coculture exhibited preferential heterotypic assembly into vascular networks in vitro, which demonstrate a stability advantage in comparison with polygonal networks of ECs alone. This model for vascular assembly should permit in vitro screening and analyses of molecules mediating assembly by selective disruption of interactions. Exploration of paracrine interactions between ASCs and EC by CM transfer demonstrated mutual chemotraction, consistent with their association in coculture. In addition, EC CM exhibited a mitogenic effect on ASCs,

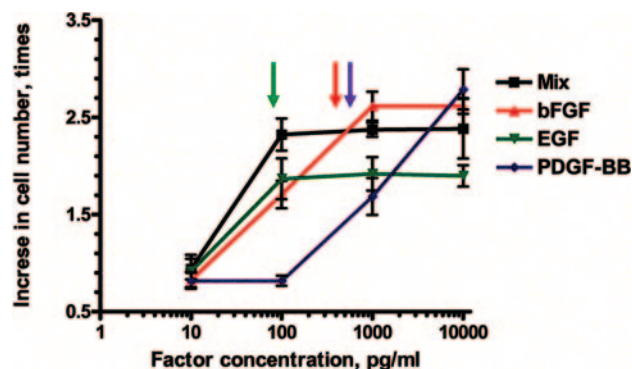


Figure 8. Mitogenic response of hASCs to bFGF, EGF, and PDGF-BB factors (known to be produced by ECs). hASCs were cultured in EBM-2/5% FBS media in the presence of 1 of bFGF, EGF, PDGF-BB, or their mixture in a range of concentrations between 10 pg/mL and 10 ng/mL for 4 days. *** $P < 0.001$. Data are presented as ratios (in percentages) of the cell counts in wells containing growth factor(s) to wells with basal media ($n = 3$). Arrows represent concentrations of factors secreted by HMVECs.

whereas ASC CM supported endothelial survival. Analysis of secreted proteins revealed candidates for mediating these responses, extending our previous description of vascular endothelial growth factor, bFGF, and hepatocyte growth factor secreted by ASCs associated with antiapoptotic effects on ECs.²⁴ Complementary factors secreted by HMVECs included isoforms of PDGF (AA, AB, and BB) as well as EGF, which showed potent mitogenic effects on ASCs, confirming functionality of PDGF receptors identified on ASCs by immunostaining. The heterotypic assembly as well as paracrine crosstalk are consistent with interactions described between microvascular ECs and pericytes from other sources.²⁷

Dual Roles for ASCs In Situ: Tissue and Vascular Support

Our findings that ASCs are components of the vascular wall functioning in paracrine support of microvasculature, complements previous understanding of their role as preadipocytes, which are able to differentiate and form new adipocytes.^{11,31} The location of the ASCs in the vessel at the interface between endothelium and adipocytes and their ability to both support vascular structure and generate adipocytes suggests a key hypothesis that they play an important role linking adipose tissue parenchymal mass with provision of its vascular supply. Indeed, forced regression of adipose tissue vasculature has been identified as an approach to reducing adipose mass.^{41,42} The novel recognition of a dual role for ASCs in adipogenesis and vascular stabilization also suggests new approaches to manipulation of adipose tissue mass.

It is tempting to speculate that this role for ASCs/pericytes in physiological vascular stabilization could underlie potential mechanisms by which exogenous ASCs enhance vascular supply and limit ischemic tissue loss in models of limb ischemia, as consistently reported.^{19,23,24,43} This has suggested that the readily available ASCs be tested as a therapy for ischemic diseases.

ASCs: Multipotent Perivascular Cells

At least 3 lines of investigation point to the notion that stem or progenitor cells in many tissues are deployed on blood vessels. Several studies have shown that pericytes isolated from different tissues are pluripotent.^{44–46} Complementary literature has suggested that MSCs are found in perivascular sites in many tissues: in bone marrow, where they interact with both sinusoidal ECs and hematopoietic precursors; in central nervous system⁴⁷; in dental pulp⁴⁸; and in others.⁴⁹ Furthermore, developmental studies have identified a perivascular mesangioblast population of dorsal aorta and other vessels that gives rise to multiple cell types, including smooth muscle cells, skeletal and cardiac muscle cells, and bone.^{50,51} The findings of our study indicate that multipotent ASCs also have a perivascular location and express pericytic markers. Analysis of all these findings suggests that in adult tissues, the perivascular compartment represents a niche for multipotent cells. The interaction of EC with these multipotent cells, including ASCs, implies that endothelium modulates their function within this niche.

We have shown that ASCs express the pericyte markers CD140a, CD140b, NG2, and α -smooth muscle actin occasionally express CD146 but lack 3G5, also a pericyte marker.^{48,52} Taking these together, it may be best to describe ASCs as a cell with pericytic properties. Without direct comparison of ASCs with pericytes from other sources, their precise relationship is difficult to assess. Also, it may be that pericytes from a range of tissues differ in antigen expression because of unique local environments. Furthermore, we would propose that pericytic identity should be primarily established by physiological properties and function rather than by surface markers.

In conclusion, the highly defined ASC population (CD34⁺/140a⁺/140b⁺/31⁻/45⁻/117⁻/144⁻) is a subset of adipose-derived cells, which in quiescent adipose tissue, possesses a majority of pericytic properties, while harboring the ability to enter into multiple other distinct lineages.

Sources of Funding

This work was supported by NIH grants R01 HL77688-01 (to K.L.M.) and T32 HL 0799905 (to D.T.) and a Veterans Affairs Merit Review grant (to K.L.M.).

Disclosures

None.

References

1. Assmus B, Schachinger V, Teupe C, Britten M, Lehmann R, Dobert N, Grunwald F, Aicher A, Urbich C, Martin H, Hoelzer D, Dimmeler S, Zeiher AM. Transplantation of Progenitor Cells and Regeneration Enhancement in Acute Myocardial Infarction (TOPCARE-AMI). *Circulation*. 2002;106:3009–3017.
2. Kawamoto A, Gwon HC, Iwaguro H, Yamaguchi JI, Uchida S, Masuda H, Silver M, Ma H, Kearney M, Isner JM, Asahara T. Therapeutic potential of ex vivo expanded endothelial progenitor cells for myocardial ischemia. *Circulation*. 2001;103:634–637.
3. Masuda H, Kalka C, Asahara T. Endothelial progenitor cells for regeneration. *Hum Cell*. 2000;13:153–160.
4. Ingram DA, Mead LE, Tanaka H, Meade V, Fenoglio A, Mortell K, Pollok K, Ferkowicz MJ, Gilley D, Yoder MC. Identification of a novel hierarchy of endothelial progenitor cells using human peripheral and umbilical cord blood. *Blood*. 2004;104:2752–2760.
5. Perin EC, Dohmann HF, Borojevic R, Silva SA, Sousa AL, Mesquita CT, Rossi MI, Carvalho AC, Dutra HS, Dohmann HJ, Silva GV, Belem L, Vivacqua R, Rangel FO, Esporcate R, Geng YJ, Vaughn WK, Assad JA, Mesquita ET, Willerson JT. Transendocardial, autologous bone marrow cell transplantation for severe, chronic ischemic heart failure. *Circulation*. 2003;107:2294–2302.
6. Prockop DJ, Sekiya I, Colter DC. Isolation and characterization of rapidly self-renewing stem cells from cultures of human marrow stromal cells. *Cytotherapy*. 2001;3:393–396.
7. Menasche P, Hagege AA, Vilquin JT, Desnos M, Abergel E, Pouzet B, Bel A, Sarateanu S, Scorsin M, Schwartz K, Bruneval P, Benbunan M, Marolleau JP, Duboc D. Autologous skeletal myoblast transplantation for severe postinfarction left ventricular dysfunction. *J Am Coll Cardiol*. 2003;41:1078–1083.
8. Menasche P, Hagege AA, Scorsin M, Pouzet B, Desnos M, Duboc D, Schwartz K, Vilquin JT, Marolleau JP. Myoblast transplantation for heart failure. *Lancet*. 2001;357:279–280.
9. Pagani FD, DerSimonian H, Zawadzka A, Wetzel K, Edge AS, Jacoby DB, Dinsmore JH, Wright S, Aretz TH, Eisen HJ, Aaronson KD. Autologous skeletal myoblasts transplanted to ischemia-damaged myocardium in humans. Histological analysis of cell survival and differentiation. *J Am Coll Cardiol*. 2003;41:879–888.
10. Goodell MA, Jackson KA, Majka SM, Mi T, Wang H, Pocius J, Hartley CJ, Majesky MW, Entman ML, Michael LH, Hirschi KK. Stem cell plasticity in muscle and bone marrow. *Ann NY Acad Sci*. 2001;938:208–218.

11. Sengenès C, Lolmede K, Zakaroff-Girard A, Busse R, Bouloumie A. Preadipocytes in the human subcutaneous adipose tissue display distinct features from the adult mesenchymal and hematopoietic stem cells. *J Cell Physiol.* 2005;205:114–122.
12. Gronthos S, Franklin DM, Leddy HA, Robey PG, Storms RW, Gimble JM. Surface protein characterization of human adipose tissue-derived stromal cells. *J Cell Physiol.* 2001;189:54–63.
13. Wickham MQ, Erickson GR, Gimble JM, Vail TP, Guilak F. Multipotent stromal cells derived from the infrapatellar fat pad of the knee. *Clin Orthop.* 2003;196–212.
14. Mizuno H, Zuk PA, Zhu M, Lorenz HP, Benhaim P, Hedrick MH. Myogenic differentiation by human processed lipoaspirate cells. *Plast Reconstr Surg.* 2002;109:199–209.
15. Zuk PA, Zhu M, Ashjian P, De Ugarte DA, Huang JI, Mizuno H, Alfonso ZC, Fraser JK, Benhaim P, Hedrick MH. Human adipose tissue is a source of multipotent stem cells. *Mol Biol Cell.* 2002;13:4279–4295.
16. Jonasson L, Hansson GK, Bondjers G, Bengtsson G, Olivecrona T. Immunohistochemical localization of lipoprotein lipase in human adipose tissue. *Atherosclerosis.* 1984;51:313–326.
17. Seo MJ, Suh SY, Bae YC, Jung JS. Differentiation of human adipose stromal cells into hepatic lineage in vitro and in vivo. *Biochem Biophys Res Commun.* 2005;328:258–264.
18. Safford KM, Hicok KC, Safford SD, Halvorsen YD, Wilkison WO, Gimble JM, Rice HE. Neurogenic differentiation of murine and human adipose-derived stromal cells. *Biochem Biophys Res Commun.* 2002;294:371–379.
19. Miranville A, Heeschen C, Sengenès C, Curat CA, Busse R, Bouloumie A. Improvement of postnatal neovascularization by human adipose tissue-derived stem cells. *Circulation.* 2004;110:349–355.
20. Cao Y, Sun Z, Liao L, Meng Y, Han Q, Zhao RC. Human adipose tissue-derived stem cells differentiate into endothelial cells in vitro and improve postnatal neovascularization in vivo. *Biochem Biophys Res Commun.* 2005;332:370–379.
21. Planat-Benard V, Menard C, Andre M, Puceat M, Perez A, Garcia-Verdugo JM, Penicaud L, Casteilla L. Spontaneous cardiomyocyte differentiation from adipose tissue stroma cells. *Circ Res.* 2004;94:223–229.
22. Strem BM, Zhu M, Alfonso Z, Daniels EJ, Schreiber R, Begyui R, MacLellan WR, Hedrick MH, Fraser JK. Expression of cardiomyocyte markers on adipose tissue-derived cells in a murine model of acute myocardial injury. *Cytotherapy.* 2005;7:282–291.
23. Planat-Benard V, Silvestre JS, Cousin B, Andre M, Nibbelink M, Tamarat R, Clergue M, Manneville C, Saillan-Barreau C, Duriez M, Tedgui A, Levy B, Penicaud L, Casteilla L. Plasticity of human adipose lineage cells toward endothelial cells: physiological and therapeutic perspectives. *Circulation.* 2004;109:656–663.
24. Rehman J, Traktuev D, Li J, Merfeld-Clauss S, Temm-Grove CJ, Bovenkerk JE, Pell CL, Johnstone BH, Conside RV, March KL. Secretion of angiogenic and antiapoptotic factors by human adipose stromal cells. *Circulation.* 2004;109:1292–1298.
25. Kang SK, Lee DH, Bae YC, Kim HK, Baik SY, Jung JS. Improvement of neurological deficits by intracerebral transplantation of human adipose tissue-derived stromal cells after cerebral ischemia in rats. *Exp Neurol.* 2003;183:355–366.
26. Nakagami H, Maeda K, Morishita R, Iguchi S, Nishikawa T, Takami Y, Kikuchi Y, Saito Y, Tamai K, Ogihara T, Kaneda Y. Novel autologous cell therapy in ischemic limb disease through growth factor secretion by cultured adipose tissue-derived stromal cells. *Arterioscler Thromb Vasc Biol.* 2005;25:2542–2547.
27. von Tell D, Armulik A, Betsholtz C. Pericytes and vascular stability. *Exp Cell Res.* 2006;312:623–629.
28. Ozerdem U, Stallcup WB. Early contribution of pericytes to angiogenic sprouting and tube formation. *Angiogenesis.* 2003;6:241–249.
29. Hughes S, Chan-Ling T. Characterization of smooth muscle cell and pericyte differentiation in the rat retina in vivo. *Invest Ophthalmol Vis Sci.* 2004;45:2795–2806.
30. Bergers G, Song S, Meyer-Morse N, Bergsland E, Hanahan D. Benefits of targeting both pericytes and endothelial cells in the tumor vasculature with kinase inhibitors. *J Clin Invest.* 2003;111:1287–1295.
31. Van Harmelen V, Rohrig K, Hauner H. Comparison of proliferation and differentiation capacity of human adipocyte precursor cells from the omental and subcutaneous adipose tissue depot of obese subjects. *Metabolism.* 2004;53:632–637.
32. Case J, Horvath TL, Howell JC, Yoder MC, March KL, Srour EF. Clonal multilineage differentiation of murine common pluripotent stem cells isolated from skeletal muscle and adipose stromal cells. *Ann NY Acad Sci.* 2005;1044:183–200.
33. Guilak F, Lott KE, Awad HA, Cao Q, Hicok KC, Fermor B, Gimble JM. Clonal analysis of the differentiation potential of human adipose-derived adult stem cells. *J Cell Physiol.* 2006;206:229–237.
34. Bunnell BA, Ylostalo J, Kang SK. Common transcriptional gene profile in neurospheres-derived from pATSCs, pBMSCs, and pNSCs. *Biochem Biophys Res Commun.* 2006;343:762–771.
35. Lee RH, Kim B, Choi I, Kim H, Choi HS, Suh K, Bae YC, Jung JS. Characterization and expression analysis of mesenchymal stem cells from human bone marrow and adipose tissue. *Cell Physiol Biochem.* 2004;14:311–324.
36. Izadpanah R, Trygg C, Patel B, Kriedt C, Dufour J, Gimble JM, Bunnell BA. Biologic properties of mesenchymal stem cells derived from bone marrow and adipose tissue. *J Cell Biochem.* 2006;99:1285–1297.
37. Muller I, Kordowich S, Spano C, Isensee G, Staiber A, Viebahn S, Giesecke F, Langer H, Gawaz M, Horwitz E, Conte P, Handgretinger R, Dominici M. Animal serum-free culture conditions for isolation and expansion of multipotent mesenchymal stromal cells from human BM. *Cytotherapy.* 2006;8:437–444.
38. Kassis I, Zangi L, Rivkin R, Levdansky L, Samuel S, Marx G, Goredetsky R. Isolation of mesenchymal stem cells from G-CSF-mobilized human peripheral blood using fibrin microbeads. *Bone Marrow Transplant.* 2006;37:967–976.
39. Igura K, Zhang X, Takahashi K, Mitsuru A, Yamaguchi S, Takashi TA. Isolation and characterization of mesenchymal progenitor cells from chorionic villi of human placenta. *Cytotherapy.* 2004;6:543–553.
40. Simmons PJ, Torok-Storb B. CD34 expression by stromal precursors in normal human adult bone marrow. *Blood.* 1991;78:2848–2853.
41. Dallabrida SM, Zurakowski D, Shih SC, Smith LE, Folkman J, Moulton KS, Rupnick MA. Adipose tissue growth and regression are regulated by angiopoietin-1. *Biochem Biophys Res Commun.* 2003;311:563–571.
42. Kolonin MG, Saha PK, Chan L, Pasqualini R, Arap W. Reversal of obesity by targeted ablation of adipose tissue. *Nat Med.* 2004;10:625–632.
43. Moon MH, Kim SY, Kim YJ, Kim SJ, Lee JB, Bae YC, Sung SM, Jung JS. Human adipose tissue-derived mesenchymal stem cells improve postnatal neovascularization in a mouse model of hindlimb ischemia. *Cell Physiol Biochem.* 2006;17:279–290.
44. Collett GD, Canfield AE. Angiogenesis and pericytes in the initiation of ectopic calcification. *Circ Res.* 2005;96:930–938.
45. Doherty MJ, Ashton BA, Walsh S, Beresford JN, Grant ME, Canfield AE. Vascular pericytes express osteogenic potential in vitro and in vivo. *J Bone Miner Res.* 1998;13:828–838.
46. Farrington-Rock C, Crofts NJ, Doherty MJ, Ashton BA, Griffin-Jones C, Canfield AE. Chondrogenic and adipogenic potential of microvascular pericytes. *Circulation.* 2004;110:2226–2232.
47. Dore-Duffy P, Katyshev A, Wang X, Van Buren E. CNS microvascular pericytes exhibit multipotential stem cell activity. *J Cereb Blood Flow Metab.* 2006;26:613–624.
48. Shi S, Gronthos S. Perivascular niche of postnatal mesenchymal stem cells in human bone marrow and dental pulp. *J Bone Miner Res.* 2003;18:696–704.
49. da Silva Meirelles L, Chagastelles PC, Nardi NB. Mesenchymal stem cells reside in virtually all post-natal organs and tissues. *J Cell Sci.* 2006;119:2204–2213.
50. Tagliafico E, Brunelli S, Bergamaschi A, De Angelis L, Scardigli R, Galli D, Battini R, Bianco P, Ferrari S, Cossu G, Ferrari S. TGFbeta/BMP activate the smooth muscle/bone differentiation programs in mesoangioblasts. *J Cell Sci.* 2004;117:4377–4388.
51. Minasi MG, Riminucci M, De Angelis L, Borello U, Berarducci B, Innocenzi A, Caprioli A, Sirabella D, Baiocchi M, De Maria R, Boratto R, Jaffredo T, Broccoli V, Bianco P, Cossu G. The meso-angioblast: a multipotent, self-renewing cell that originates from the dorsal aorta and differentiates into most mesodermal tissues. *Development.* 2002;129:2773–2783.
52. Nayak RC, Berman AB, George KL, Eisenbarth GS, King GL. A monoclonal antibody (3G5)-defined ganglioside antigen is expressed on the cell surface of microvascular pericytes. *J Exp Med.* 1988;167:1003–1015.

Online Data Supplements

Expanded Materials and Methods

Immunofluorescent analysis of adipose tissue

Human fat was mounted in OCT medium (Fisher, Hampton, NH) and frozen in liquid N₂. 20 µm sections were prepared, acetone fixed for 5 minutes and treated with protein block solution (Dako, Carpinteria, CA) for 20 minutes. Adipose tissue was stained with rabbit anti-CD31 (LabVision, Fremont, CA, dilution 1:100) together with mouse anti-human CD34 (BD Pharmingen, 1:50), or with mouse anti-human CD31 (LabVision, dilution 1:100) together with rabbit anti-CD140b (LabVision) antibodies. All primary antibodies were incubated for 1 hour at room temperature. To detect primary antibodies, goat anti-rabbit Alexa 546 and chicken anti-mouse Alexa 488 antibodies (Molecular Probes, Eugene, OR) were applied for 30 minutes. The nuclei were counterstained with DAPI. Slides were observed and pictures were recorded using a Zeiss LSM 510 confocal microscope.

Immunofluorescent analysis of isolated adipose stromal cells

Freshly isolated adipose stromal cells were plated on cell culture plastic. Non-attached cells were washed off at day 1. At day 2 cells were harvested with 0.05% Trypsin/EDTA and re-plated onto cover glasses coated with rat tail collagen (BD, San Diego, CA). Cells were allowed to attach overnight and washed with PBS followed by 10 min fixation in 4% formaldehyde. To permeabilize cell membranes, slides were treated with 0.1% Triton X-100. Nonspecific binding of antibodies was decreased by exposure to protein block (Dako Cytomation, Carpinteria, CA) for 20 min. Cells were incubated

with primary mouse antibodies against caldesmon, calponin (all 1:200, all Santa Cruz, Santa Cruz, CA) and α -smooth muscle actin (1:1000, Sigma, St. Louis, MO) for 1 hour. As control for nonspecific staining, the same concentrations of nonimmune mouse monoclonal IgG were used. For fluorescent visualization of the antibody reactions anti-mouse IgG Alexa Fluor 488 labeled secondary antibodies (1:200; Invitrogen, Carlsbad, CA) were used. The nuclei were stained with DAPI.

Analysis of factor accumulation in conditioned media of hASC and HmVEC

Freshly isolated hASC, or HmVEC (passage 7), were plated overnight on cell culture plastic in EBM-2/5%FBS. All non-attached cells were washed off, attached cells were harvested with 0.05% Trypsin/EDTA and re-plated into T25 culture flasks with EBM-2/5%FBS at a density of 60×10^3 cell/cm². The following day the media was exchanged to fresh EBM-2/5%FBS and cells were cultured for 72 h. The conditioned media were analyzed for the accumulation of growth factors, cytokines and other bioactive molecules using RayBiotech Cytokine Antibody Arrays VI and VII for hASC and RayBiotech Growth Factor Antibody Arrays I for HmVEC (RayBiotech Inc) according to the manufacturer instructions.

Quantitative assessment of growth factors accumulated in HmVEC-conditioned media

Concentrations of human bFGF, human EGF and human PDGF-BB accumulated in media conditioned by HmVEC for 72 hours were evaluated using Pierce Biotech "Searchlight" technology.

Evaluation of hASCs antigens by PCR

ASC cultured for two days on standard cell culture plastic were sorted with an Aria Cell Sorter (Becton Dickinson Immunocytometry Systems), selecting for the cell surface marker profile CD31⁻/CD45⁻/CD34⁺/CD140b⁺. Total cellular RNA was isolated from purified ASC populations using RNase Miniprep Kit (Qiagen) followed by a reverse transcription reaction with the Omniscript RT kit (Qiagen). Polymerase chain reactions (PCR) were performed using SYBR Green PCR Master Mix (Applied Biosystems). PCRs were performed in a final volume of 25 µl reaction mix that contained 50 ng of cDNA product, 200 nmol/L of each primer. For all reactions thermal cycling parameters were: 10 minutes at 95°C for AmpliTaq Gold activation followed by 40 cycles of 15 seconds at 95°C for denaturation and 1 minute at 60°C for anneal/extend. The oligonucleotides used as primers are presented in the supplemental table I.

Table I: Sequence of primers used for PCR reaction.

Antigen	Sense strand	Anti-sense strand	band size
CD10	5'-AGATAGTCTTCCCAGCCGGC-3'	5'-AAGCCATGGGTGATTTGCGT-3'	115 bp
αSMA	5'-GATCTGGCTGGCCGAGATC-3'	5'-ATGTCCCGGACAATCTCACG-3'	115 bp
CD144	5'-CACGCCTCTGTCATGTACCAA-3'	5'-CGATCTCATACTGGCCTGC-3'	121 bp
CD31	5'-TCATTTCTGGGATCCATATGCA-3'	5'-TGGGTGTAGAGAAGGATTCCGT-3'	81 bp
CD90	5'-CTGGCCATCAGCATCGCT-3'	5'-TATTCTCATGGCGGCAGTCC-3'	121 bp
Caldesmon	5'-AAGAATCCTTGGGACAGGTGAC	5'-GTGGTGGTTGTCTTGGCCTC-3'	115 bp
CD34	CAAGATGTTGCAAGCCACCA	5'-AGGAAATAGCCAGTGATGCCC-3'	101 bp
CD140a	5' – AGAGGAGCATTTGGAGTGCG - 3'	5' – CCGTGTCTCTTCCCATAAT - 3'	68 bp
CD140b	5' – TATGCCTTACCACATCCGCTC - 3'	5' – TCACACTCTCCGTACATTGC - 3'	92 bp
CD13	5' – TTGGACCAAAGTAAAGCGTGG - 3'	5' – TACGGTCTCAGCGTCACCTG - 3'	83 bp
NG2	5'-CCAGGAAAGGCAACCTTCAAC-3'	5'-ACGGAAACGGAAGGTGTCC-3'	142 bp

Xenograft Transplantation

Cellularized gel implants were cast as previously described by Schechner, J.S. et al., (2000) with minor modifications. Defined mixtures of HUVEC and ASC (4:1) were suspended in solution containing 1.5 mg/ml rat-tail collagen I, 100 ng/ml human fibronectin (Chemicon), 1.5 mg/ml sodium bicarbonate (Sigma), 25 mM HEPES (Cambrex), 10% FBS, and 30% EGM-2/10%FBS, in EBM-2 at a final concentration 2×10^6 total cells/ml. The cell suspensions were placed in a 12-well tissue culture dish (1 ml/well) for 30 minutes at 37°C for polymerization, and incubated under EGM-2/10%FBS overnight. The following day, gels (500 μ l) were implanted subcutaneously on the abdominal wall muscle of anesthetized 8-12 weeks old nude mice (Harlan, Indianapolis, IN). Fourteen days after transplantation, the implants were excised and preserved for immunohistochemical evaluation. All experiments were approved by the Indiana University Laboratory Animal Research Center.

Immunohistochemical evaluation of collagen implants

After excision, implants were immersed in 4% formaldehyde, followed by paraffin embedding and staining for vascular structures using antibodies against CD31 and α -smooth muscle actin. Deparaffinized sections were boiled in Citrate Retrieval buffer (20 min) and incubated with protein block solution (Dako, Carpinteria, CA) for 20 minutes. Sections were incubated with rabbit anti-CD31 IgGs (Lab Vision, Fremont, CA, 1:100) and mouse α -smooth muscle actin IgGs (Sigma, 1:800). To detect primary antibodies, sections were incubated with goat anti-rabbit Alexa 546 (Invitrogen, A11035, 1:200) and

chicken anti-mouse Alexa488 (Invitrogen, A21200; 1:200) IgG for 30 minutes. The nuclei were counterstained with DAPI.

Differentiation of ASC into mesenchymal cell types.

Populations of ASC were sorted 2 days following plating for the phenotypic profile CD45-/CD31-/CD34+/CD140b+, expanded for 1 passage, and then evaluated for differentiation capacity as follows.

Adipogenic differentiation. Cells were plated on plastic at a density of $5 \times 10^4/\text{cm}^2$ and allowed to attach overnight in EBM-2/5%FBS media, after which the media were replaced with preadipogenic or adipogenic differentiation media (Zen-Bio, Research Triangle Park, NC). The latter media were changed after 4 days. The degree of adipogenic differentiation was evaluated at day 8 by staining cell monolayers with Nile red or against FABP-4 protein. ASC monolayers were fixed with 4% paraformaldehyde, followed by incubation with 10 $\mu\text{g}/\text{ml}$ Nile Red for 20 min at room temperature. Between the steps cells were washed 3 times with PBS. Nile Red accumulation was evaluated using a Triad Multimode Plate Reader (DYNEX Technologies, Inc.; Chantilly, VA, USA) with filter settings: Ex- 485 nm, Em – 535 nm. Formalin-fixed monolayers of ASC were incubated with goat anti-mouse FABP-4 (R&D Systems, Minneapolis, MN) overnight at 4 °C, followed by incubation with chicken anti goat Alexa 488 (Molecular Probes, dilution 1:200). Nuclei were visualized by DAPI staining.

Osteogenic differentiation. Cells were plated on fibronectin-coated plastic at a density of $3 \times 10^4/\text{cm}^2$ and allowed to attach overnight in EBM-2/5%FBS media. The next morning, media were replaced by fresh EBM-2/5%FBS or Osteogenic Differentiation

media provided within the Stem Cell kit (R&D Systems). Media were changed every 4 days. Osteogenic differentiation was confirmed by Alizarin Red staining for visualization of calcification. ASC monolayers were fixed with 10% formalin for 1h, followed by incubation with 0.5% Alizarin Red (pH 4.1) for 5 min.

Statistical analysis

Wherever possible, data are expressed as mean \pm s.e.m. Comparisons between mitogenic responses to growth factors were performed with a paired t-test. Experiments were repeated 3 times with 3 different patient samples. Analysis was performed using Prism 4 (Graphpad, San Diego, CA).

Figure legends

Figure I. Differentiation of marker-purified hASC into adipocytes.

ASC purified by sorting for the phenotype CD31⁻/CD45⁻/CD34⁺/CD140b⁺ were exposed to adipogenic differentiation media for 8 days. (A) Representative photos of fluorescent staining of control and differentiated ASC monolayers exposed to Nile Red dye (FITC channel) and immunofluorescent staining against FABP-4 antigen confirm adipogenic differentiation; (B) Quantitative evaluation of Nile Red accumulation into lipid in control and differentiated ASC. Measurements were made using Triad Multimode Plate Reader (DYNEX Technologies, Inc.; Chantilly, VA, USA) with excitation at 535 nm and emission at 595 nm.

Figure II. Differentiation of marker-purified hASC into osteoblasts.

ASC purified by sorting for the phenotype CD31⁻/CD45⁻/CD34⁺/CD140b⁺ were exposed to osteogenic differentiation media for 21 days. (A) Representative photos of control and differentiated ASC staining with Alizarin Red reveal mineralization upon stimulation.

Figure III. PCR analysis of marker-purified CD34+ adipose stromal cells to confirm expression of endothelial, mesenchymal and pericyte markers. hASC were sorted to obtain a purified population defined by the markers CD31⁻/CD45⁻/CD34⁺/CD140b⁺. RT-PCR was then performed with RNA samples purified from HmVEC (passage 7), or hASC sorted as indicated two days following plating.

Figure IV. Histological analysis of Collagen gels vessels development. Formalin-fixed paraffin-embedded sections of collagen gels were stained with antibodies against HUVEC (CD31, green) and ASC / pericyte (α SMA, red) markers, or with corresponding isotype control IgGs. Cell nuclei are revealed by DAPI staining.

Figure V. Analysis of bioactive molecules accumulated in media conditioned by hASC (A) or HmVEC (B). hASC or HmVEC were cultured in EBM-2/5%FBS media for 72 hours. Analysis was performed utilizing RayBio membranes VI and VII (for hASC) and RayBio Growth Factor Antibody Arrays I (for HmVEC) (n=3). The rectangular

frames highlight factors that have direct effects on angiogenesis and are not present in control arrays (incubated with EBM-2/5%FBS).

Fig S1.

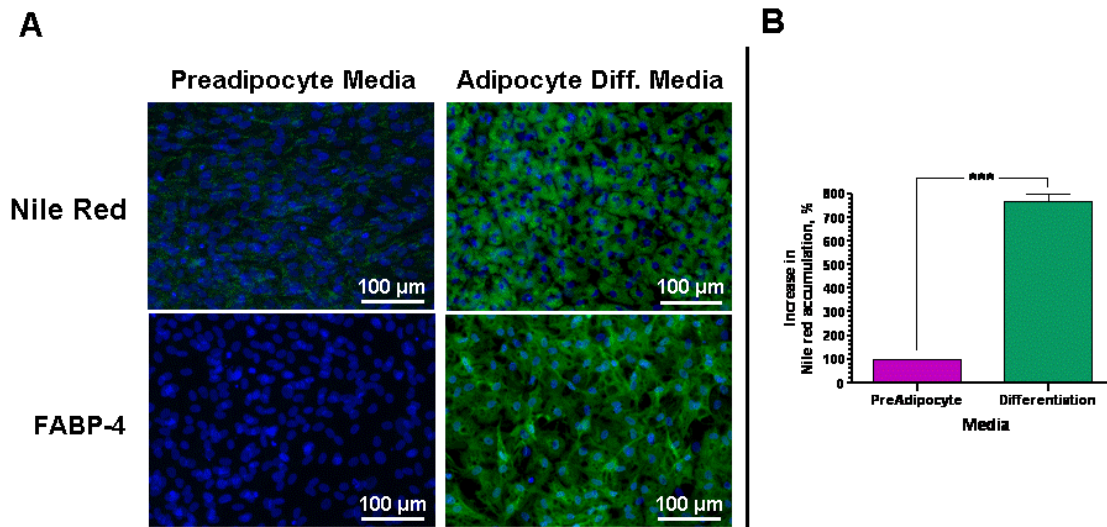


Fig S2.

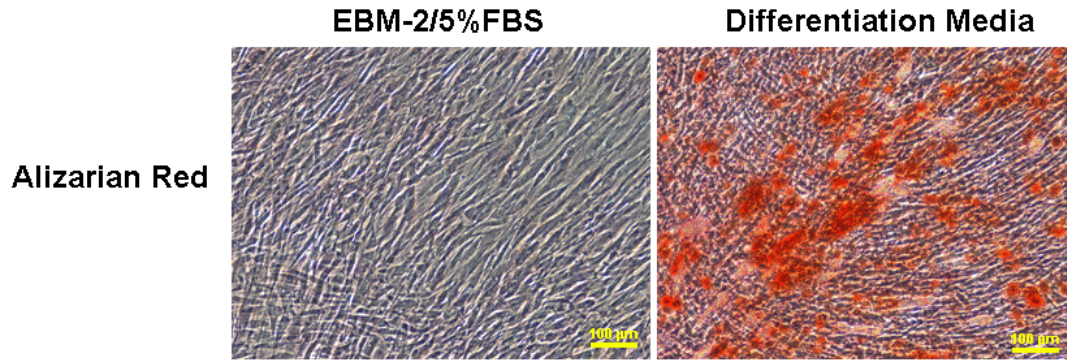


Fig S3.

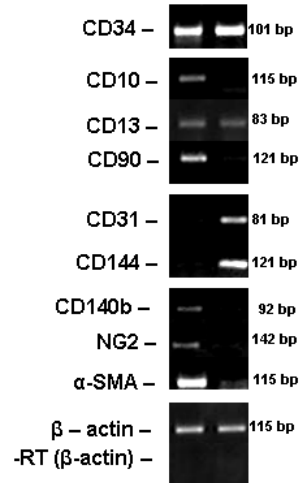


Fig S4.

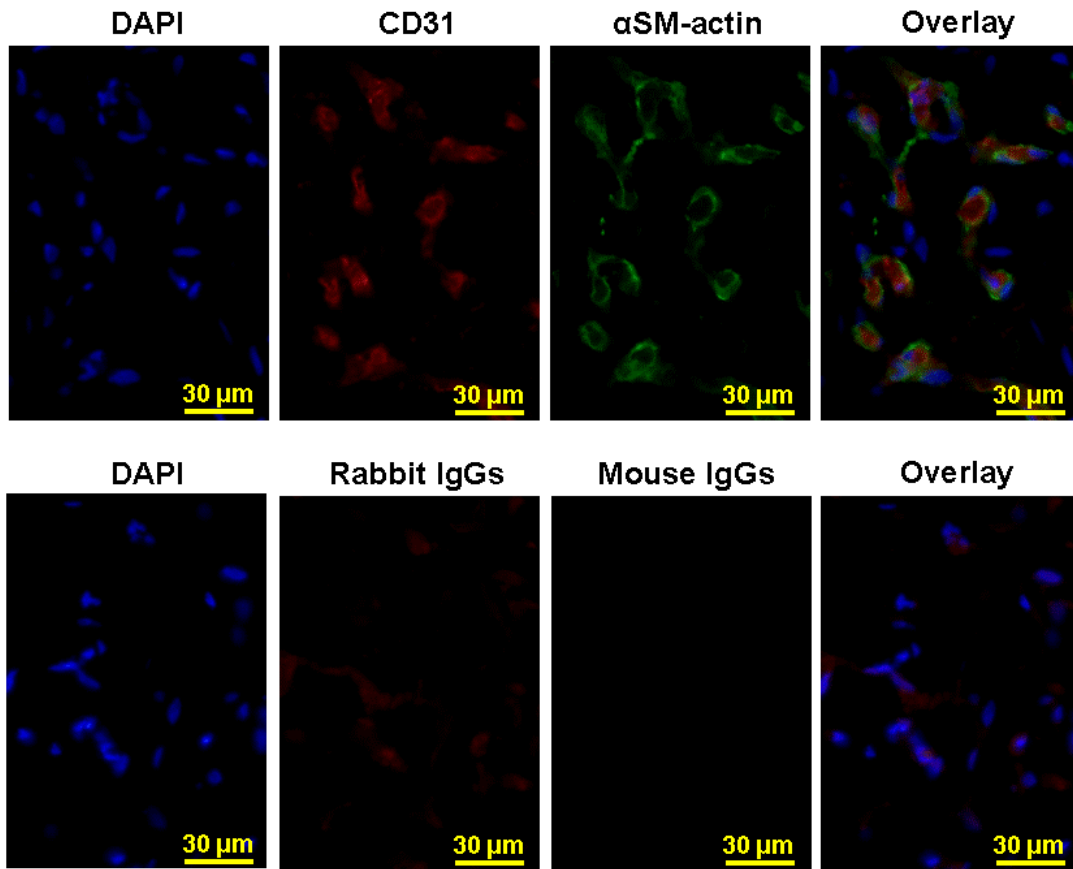


Fig S5.

